Slovak Geol. Mag., 9, 1(2003), 51 – 64

Manganese mineralization near Šarišské Jastrabie village, Pieniny Klippen Belt, Western Carpathians, Slovakia

IGOR ROJKOVIČ, LADISLAVA OŽVOLDOVÁ and MILAN SÝKORA

Faculty of Nature Sciences, Comenius University, Mlynská dolina, 842 15 Bratislava, Slovak republic
e-mail: rojkovic@fns.uniba.sk

Abstract. Manganese mineralization is located in shale and radiolarite chert of Kysuca Formation of the Klippen Belt. Late Bathonian – Early Callovian (U.A.Z.7) shale is underlying in tectonic contact Middle Callovian- Early Kimmeridgian (U.A.Z. 8 – U.A.Z. 10) radiolarite chert. Layers with rhodochrosite (5 to 20 cm thick) are bound to shale. Manganese oxides and hydroxides form secondary crusts on layers with rhodochrosite and fill fissures in radiolarite chert. They are represented by pyrolusite, cryptomelane, romanèchite, todorokite and they are accompanied by goethite. Primary manganese carbonates were formed probably during diagenesis. Secondary manganese oxides and hydroxides were formed in shale and radiolarite chert during weathering processes.

Key words: Manganese minerals, radiolarians, Kysuca formation, Klippen Belt, Western Carpathians

Introduction

Several deposits of a manganese are known ore in the Jurassic radiolarite chert Late Jurassic up to Cretaceous chert in California contains lenses with manganese ore closely associated with basalt (Crerar et al., 1982). Jurassic chert with manganese ore overlying basalt occurs in Apennine peninsula (Bonatti et al., 1976). These deposits were formed in sea bottom by hydrothermal fluids related to volcanic activity.

Manganese ore occurs in the Middle to Upper Jurassic sequences of the Pieniny Klippen Belt of the Kysuca Succession in Eastern Slovakia near the eastern margin of Šarišské Jastrabie village (Fig. 1). The early prospecting for manganese started in the 19th century. Later attempts to mine the ore followed during the First and the Second World War. New adit of NW direction was opened in 1941.

Manganese ore occurs according to Ilavský (1955) in bed 10 up to 40 cm thick bound to lower - most part of radiolarite chert overlying greyish green shale in the valley of Vesné brook. Lenticular nodules with dark manganese oxides were observed also near the contact (up to 30 cm) in the underlying shale. Farther from the contact the manganese oxides have not been observed.

Average chemical composition of ore according to Ilavský (1955) is: Mn 18,9 %, Fe 15,23 %, S 0,16 %, SiO_2 30,6 % and Al_2O_3 14,11 %. Primary ore is formed by manganese carbonate (rhodochrosite-dialogite) with crusts of psilomelane or wad and limonite stains. Chemical composition, microscopic observations and geological position led Ilavský (1955) to assumption of secondary origin of manganese mineralization by leaching from radiolarite chert and accumulation of manganese minerals on the base of radiolarite chert overlying the impermeable shale.

Geological setting

The Pieniny Klippen Belt is an extremely complicated tectonic zone of the Carpathians. It is a narrow belt spreading over 400 km in Slovakia from Záhorská nížina plain in the West to the border with Ukraine in the East. It is mostly several kilometres wide with maximum 15 km near the town Púchov. The Klippen Belt represents tectonic boundary between Outer Carpathians on the north and the Inner Carpathians on the south. It is formed by the Jurassic, Cretaceous and Paleogene sequences.

An investigated area belongs to the eastern part of the Pieniny Klippen Belt. Formations with manganese mineralization are bound to the klippes of the Kysuca Succession – equivalent of the Branisko Succession in Poland. These are surrounded by Paleocene to Eocene formations represented by red and green shale and sandstone (Nemčok 1990, Nemčok et al. 1990)

Birkenmajer (1977) introduced a term Sokolica Radiolarite Formation for Middle and Late Jurassic sequences with coatings of manganese mineralization in Pieniny, Branisko and Magura Successions. Birkenmajer (1977) supposed Upper Bajocian (?) to Callovian and Lower Oxfordian (?) for this formation. An original name of this formation was „manganese radiolarites" (Birkenmajer 1954, 1958). Rocks are represented by thin-bedded greyish green, greyish blue and black radiolarites alternating with similarly coloured siliceous shale. The lowermost part of this formation is represented by the shale and the limestone also bearing manganese mineralization. The Sokolica Radiolarite Formation was defined for the formation of radiolarite and shale with manganese mineralization without respect to a primary origin of the manganese mineralization.

Slovak Geol. Mag., 9, 1(2003), 51 – 64

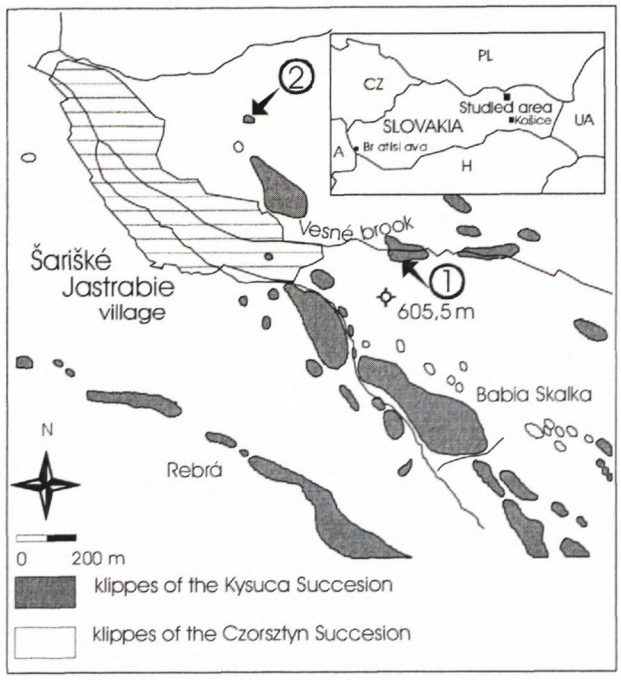

Fig. 1. Occurrences of manganese mineralization near Šarišské Jastrabie village. Localities: 1 – Vesné Brook, 2 – Quarry.

Overlying Czajakowa Radiolarite Formation of the Lower Oxfordian to Lower Kimmeridgian age (Birkenmajer 1977) is represented by green, grey or green-red stripped radiolarite chert in the lower part and by red radiolarite chert in the upper part. The manganese mineralization is absent in these rocks.

Position of outcrops

1. Vesné Brook

Klippe of a lenticular shape is situated in stream bed, 200 meters to the east from Šarišské Jastrabie village and 150 meters NNW from the elevation point 605,5 meters (Fig. 1). The klippe of Kysuca Succesion consists of Sokolica Radiolarite Formation and Czajakowa Radiolarite Formation (Birkenmajer 1977). The thickness of both formations in the outcrop is about 6 m. Strike of radiolarite chert beds is 340 – 350/10 – 20° to the west. Lower part of Sokolica Radiolarite Formation represented by shale is separated from radiolarite chert in upper part of formation by fault striking 60/25° to SSE (Fig. 2). Layers and boudinage of rhodochrosite can be seen in outcrop (Fig. 3). Dump of mined adit for Mn – ore from the first half of the 20th century is located nearby the outcrop, some 70 m NNW from the northern margin of the village.

2. Quarry

A small quarry in the same formation as in the first locality is situated 120 m NE from cemetery. The outcrop consists of sediments the Czajakowa Radiolarite Formation (Birkenmajer, 1977) 3 to 4 m in thickness striking 60/15° to SSE. Radiolarite chert of Sokolica Radiolarite Formation (Birkenmajer, 1977) with manganese coatings can be seen in small thickness only (less than 1 m). The same shale as in previous outcrop is separated from radiolarite chert by fault striking 20/55° to W (Fig. 4).

Lithologic characteristic

1. Vesné Brook:

Czajakowa Radiolarite Formation is composed of radiolarite chert layers (10 to 25 cm thick) with alternation of red and green strips. The upper part of radiolarite chert is dominantly of red colour. Spherical as well as three rayed tests of radiolarians (0,1 to 0,2 mm across) are frequent. Originally opal tests were transformed to quartz often with radial structure or they were dissolved and gradually filled up by calcite. Radiolarians represent up to 25 vol. % of rock in thin sections. Less distinct parallel lamination is hardly observed. Clastic quartz and mica are rare. Radiolarite chert of Sokolica Radiolarite Formation is mostly grey-green with coatings of manganese minerals. Radiolarite chert is near the tectonic contact with underlying shale brecciated and cemented by calcite.

Underlying shale of the Sokolica Radiolarite Formation is characterized by prevailing illite. There are also clastic anhedral quartz grains, micas, oval clasts of shale, altered clastic feldspars and fragments of plant tissue. Rare accessory zircon and rutile were also observed. Seldom tests of radiolarians, spores of pteridophyte ferns or fungi are also present. Cysts of dinoflagellates genus *Hystrichosphaeridium* in sample 17 were identified. Clastic minerals form less distinct lamination of shale (Fig. 5).

Shale alternates with layers or boudinage of pale brown carbonates (up to 20 cm thick) with dominant rhodochrosite (0,015 to 0,03 mm in size). Carbonates contain pseudomorphs after spherical radiolarians (Fig. 6). They are filled with rhombohedrons of rhodochrosite, fine-grained quartz and chlorite. Lithoclasts of siltstone (1 to 2 mm in size) with pelitic matrix were found also in carbonates. Manganese oxide and hydroxide coatings cover layers and boudinage of rhodochrosite. The other sediments of the Sokolica Radiolarite Formation as siliceous shales and grey-green spotted siliceous limestone described by Mycziński (1973) have not been found.

2. *Quarry*

The western part of quarry is mainly represented by the Czajakowa Radiolarite Formation with intercalation of siliceous shale (Ožvoldová & Frantová, 1997), which is overlaid by Tithonian to Lower Cretaceous light grey radiolarian limestone with rare silicified belemnites (Pieniny Limestone Formation). The fissures in underlying radiolarite chert of the Sokolica Radiolarite Formation are coated with manganese oxides and hydroxides.

Carbonate layers (5 to 10 cm thick) with manganese oxides and hydroxides can be observed in shale in the eastern part of the quarry. Shale consists of illite, chlorite and rare clastic quartz (0,02 to 0,05 mm in size). Shale

Fig. 2. Outcrop of radiolarite (in left) and shale (in right) in Vesné Brook, Šarišské Jastrabie. Symbols: radiolarite (circle), shale (square) and boudinage with rhodochrosite (star). Fault is marked with dashed line.

Fig. 3. Layer and boudinage (up) of carbonates in shale. Vesné brook, 5 m NW from tectonic contact on Fig. 2. Symbols: radiolarite (circle), shale (square) layer and boudinage with rhodochrosite (star).

contains disseminated coal plant fragments and rare fish teeth. Some samples show brecciated texture and cracks filled by polycrystalline quartz.

Radiolarian microfauna

Radiolarian microfauna was studied especially in shale and its tectonic contact with overlying radiolarite. The samples, taken from radiolarite were used to complement data to the established age by Ožvoldová & Frantová (1997). Shale samples were treated with 12 % acetic acid and 5 % HF (1-2 days), radiolarite samples using standard HF method as well. Dating of radiolarian microfauna is based on the biozonation of Baumgartner et al. (1995). The position of all samples is shown on the Fig. 2, 3 and 4. Distribution of radiolarians in the samples, containing radiolarian microfauna is demonstrated in Tab. 1. Illustration of important species is shown in Fig. 7, 8.

Vesné brook

Radiolarite of Czajakowa Radiolarite Formation, in the upper part of the sequence, of rusty red colour, without Mn coatings contains the assemblages, which represent U.A.Z. 9 – U.A.Z. 10 (Middle Oxfordian to Late Oxfordian - Early Kimmeridgian) (Ožvoldová & Frantová, 1997). This stratigraphical range was confirmed by our investigation (sample ŠJ 6), based on the occurrence of the species *Podocapsa amphitreptera* Foreman, *Fultacapsa sphaerica* (Ožvoldová), *Angulobracchia biordinalis* Ožvoldová and *Paronaella broennimanni* Pessagno.

Underlying layers of this formation, of greenish grey or greyish green colour contains assemblages, represent-

Slovak Geol. Mag., 9, 1(2003), 51 – 64

Fig. 4. Outcrop of radiolarite (in left) and shale (in right) in quarry NE from cemetery. Explanations: radiolarite (circle), shale (square) and layer with rhodochrosite (star). Fault is marked with dashed line.

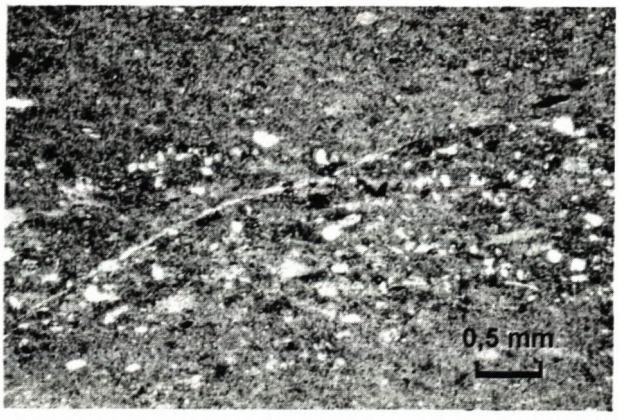

Fig. 5. Shale with band of clastic quartz (parallel to longer size of the figure). ŠJ 8, parallel nicols..

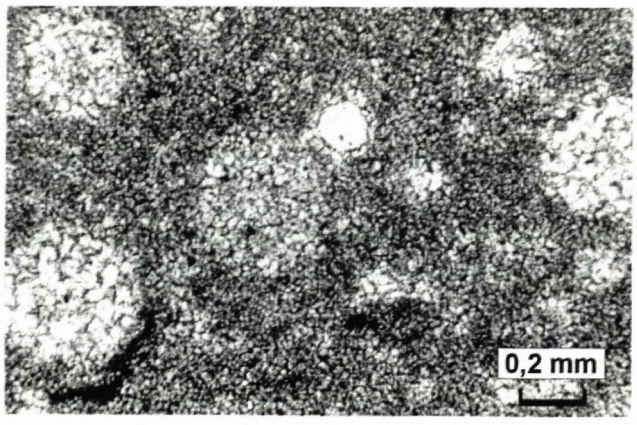

Fig. 6. Aggregates of rhodochrosite are dominant in rock. Carbonates and quartz (white) replace spherical radiolarians. ŠJ 2, transmitted light, parallel nicols.

ing Unitary Association Zone 8 (U.A.Z. 8) (l.c.), which stratigraphical range is Middle Callovian - Early Oxfordian.

Radiolarite with manganese coatings (Sokolica Radiolarite Formation) yields badly preserved assemblages. The presence of the species *Eucyrtidiellum ptyctum* Riedel et Sanfilippo, which, according recent research in the Pieniny Klippen Belt does not appear before Callovian, proves, that this part of sequence is not older than Callovian (Ožvoldová & Frantová, 1997).

Shale sequence, separated from overlying radiolarite by a tectonic contact, contained very poor microfauna, preserved mostly in phantoms (sample ŠJ 9). Determinable specimens were *Transhsuum brevicostatum* (Ožvoldová), *Paronaella* cf. *pristidentata* Baumgartner, *and Tricolocapsa* sp., *Paronella* sp. Its assemblage refers to Middle – Upper Jurassic age. The lower and upper boundary is restricted by the species *Transhsuum brevicostatum* (Ožvoldová), which appears in Bajocian and extincted in Tithonian.

The assemblage in the sample ŠJ 10 with the species *Kilinora spiralis* (Matsuoka), *Cinguloturris carpatica* Dumitrica, *Mirifusus dianae* (Karrer) and *Stichocapsa robusta* Matsuoka corresponds to U.A.Z. 7 and the stratigraphical range Late Bathonian to Early Callovian. In a comparison with the other analysed associations of this range in the Pieniny Klippen Belt (Ožvoldová, in preparation) it represents the upper part of this stratigraphical range.

Tab. 1. Distribution of radiolarians in the studied samples

Radiolarian fauna	Sample				
	ŠJ 6	ŠJ 9	ŠJ 10	ŠJ16	ŠJ25
Angulobracchia biordinalis Ožvoldová	*				
Angulobracchia digitata Baumgartner			*		
Angulobracchia sp.					*
Archaeospongoprunum imlayi Pessagno	*			*	
Cinguloturris carpatica Dumitrică			*	*	*
Deviatus diamphidius hipposidericus (Foreman)				*	
Emiluvia ordinaria Ožvoldová	*			*	
Emiluvia pessagnoi Foreman	*				
Emiluvia premyogii Baumgartner	*				
Emiluvia salensis Pessagno	*		*		
Emiluvia sedecimporata (Rüst)	*				
Fultacapsa sphaerica (Ožvoldová)	*			*	
Eucyrtidiellum sp.					*
Haliodictya (?) antiqua (Rüst)			*		
Higumastra imbricata (Ožvoldová)			*		
Homoeoparonaella argolidensis Baumgartner	*				
Homoeparonaella sp.					*
Kilinora spiralis (Matsuoka)			*		
Mirifusus dianae (Karrer)	*		*	*	
Mirifusus guadalupensis Pessagno					*
Napora lospensis Pessagno	*				
Obesacapsula cf. morroensis Pessagno	*		*		*
Palinandromeda podbielensis (Ožvoldová)			*		
Paronaella broennimanni Pessagno	*			*	
Paronaella pristidentata Baumgartner				*	
Paronaella cf. pristidentata Baumgartner		*			
Paronaella sp.		*			
Parvicingula dhimenaensis Baumgartner	*				
Podobursa spinosa (Ožvoldová)					
Podobursa triacantha (Fischli)					
Podocapsa amphitreptera Foreman	*			*	
Protunuma japonicus Matsuoka et Yao					*
Pseudoctrucella sanfilippoae (Pessagno)					*
Sethocapsa funatoensis Aita					*
Spongocapsula palmerae Pessagno	*				
Stichocapsa robusta Matsuoka			*		
Tetraditryma corralitosensis (Pessagno)			*		
Tetraditryma pseudoplena Baumgartner			*		
Tetratrabs zealis (Ožvoldová)			*		
Transhsuum brevicostatum (Ožvoldová)		*	*	*	
Transhsuum maxwelli (Pessagno)			*		*
Triactoma blakei (Pessagno)	*			*	
Triactoma jonesi (Pessagno)			*		
Tricolocapsa sp.		*			
Tritrabs ewingi (Pessagno)			*		
Tritrabs rhododactylus Baumgartner			*	*	
Zhamoidellum ovum Dumitrică	*			*	

Quarry

Radiolarite sequence is predominantly formed by the radiolarite of Czajakowa Radiolarite Formation containing microfauna, which represents U.A.Z. 9 – U.A.Z. 10 - Middle Oxfordian to Late Oxfordian – Early Kimmeridgian (Ožvoldová & Frantová, 1997).

Radiolarite with Mn coatings of Sokolica Radiolarite Formation, which occurs in a small amount yields microfauna (ŠJ 16), in which the presence of the species *Paronaella pristidentata* Baumgartner and Paronaella *broennimanni* Pessagno indicates U.A.Z. 10 – Late Oxfordian – Early Kimmeridgian. This fact confirms the datum of Ožvoldová & Frantová (1997), that the manganese coatings in radiolarite extend somewhere up to Middle – Late Oxfordian.

Shale sequence contains badly preserved microfauna (ŠJ 25,) with the species of a relatively broad stratigraphical range. It can be assigned to the U.A. zones U.A.Z. 7 – U.A.Z. 10 – Late Bathonian - Early Callovian to Late Oxfordian-Early Kimmeridgian, based on the presence of the species *Protunuma japonicus* Matsuoka et Yao and Pseudocrucella *sanfilippoae* (Pessagno). However, it is likely, that the age is not different from the samples in the Vesné Brook (ŠJ 9, ŠJ 10).

The studied sections the shale sequence with Mn coatings, occurring in the lower part of the sections and belonging according to Birkenmajer (1977) to Sokolica Radiolarite Formation contained a radiolarian microfauna, representing U.A.Z. 7 - Late Bathonian – Early Callovian.

Radiolarite sequence overlying shale at the both outcrops yielded the assemblages corresponding to the U.A.Z.8 – U.A.Z. 10 with the stratigraphical range-Middle Callovian - Early Oxfordian to Late Oxfordian - Early Kimmeridgian. Radiolarite with Mn coatings, which formed according to Birkenmajer (1977) Sokolica Radiolarite Formation reaches somewhere up to Middle – Late Oxfordian.

Manganese mineralization

Manganese ore represented in both localities by rhodochrosite forms intercalations and boudinage in shale and it is not bound to basal part of the radiolarite chert as described by Ilavský (1955). Secondary manganese oxides and hydroxides form crusts on rhodochrosite layers (Fig. 9) and they also fill the fissure in the overlying radiolarite chert close to the tectonic contact (Fig. 10).

Methods

Identification of minerals, distribution o elements and chemical composition of minerals was analysed by wave-dispersion X-ray microanalysis (WDX), energy-dispersion X-ray microanalysis (EDX) and by X-ray diffraction analysis (XRD). WDS analyses were carried out on a JEOL-733 Superprobe equipped with KEVEX Delta IV+ energy disperse system (Geological Survey of Slovak Republic). Analysed elements were Al, Ba, Ca, Fe,

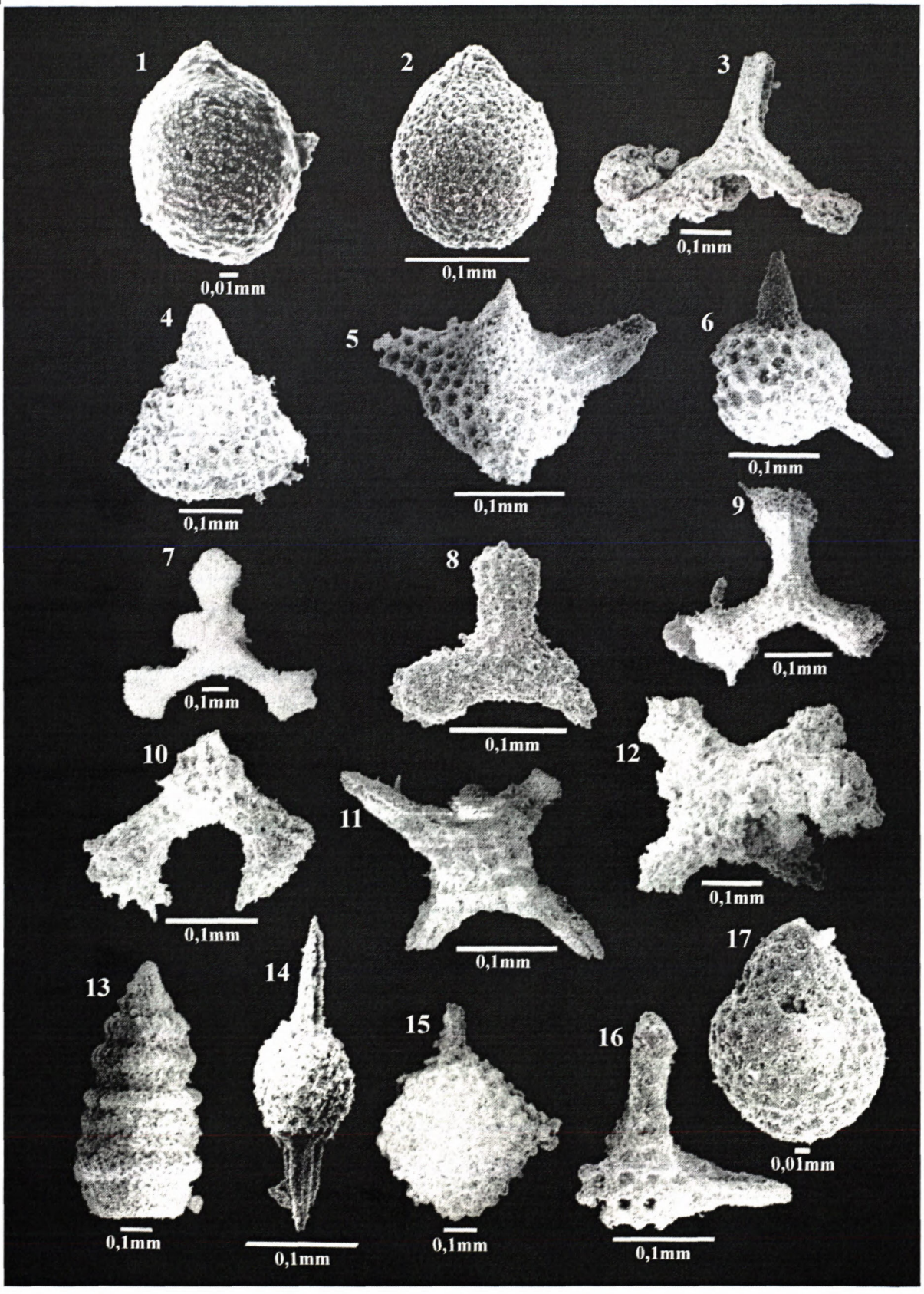

Fig. 7. 1 – Kilinora spiralis (Matsuoka) – 1309, ŠJ – 10, 2 – Stichocapsa robusta Matsuoka – 1306, ŠJ – 10, 3 – Angulobracchia digitata Baumgartner – 1312, ŠJ – 10, 4 – Palinandromeda podbielensis (Ožvoldová) – 1304, ŠJ – 10, 5 – Podocapsa amphitreptera Foreman – 1334, ŠJ – 16, 6 – Fultacapsa sphaerica (Ožvoldová) – 1339, ŠJ – 16, 7 – Angulobracchia biordinalis (Ožvoldová) – 7906, ŠJ – 6, 8 – Paronaella pristidentata Baumgartner – 1342, ŠJ – 16, 9 – Paronaella broennimanni Pessagno – 1326, ŠJ – 16, 10 – Deviatus diamphidius hipposidericus (Foreman) – 1340, ŠJ – 16 , 11 – Emiluvia sedecimporata (Rüst) – 1344, ŠJ – 6, 12 – Higumastra imbricata (Ožvoldová) – 1325, ŠJ – 10, 13 – Cinguloturris carpatica Dumitrică – 1346, ŠJ – 16, 14 – Archaeospongoprunum imlayi Pessagno – 1335, ŠJ – 16, 15 - Emiluvia pessagnoi Foreman – 7909, ŠJ – 6, 16 – Emiluvia ordinaria Ožvoldová - 1336, ŠJ – 16, 17 – Zhamoidellum ovum Dumitrică – 1345, ŠJ – 16.

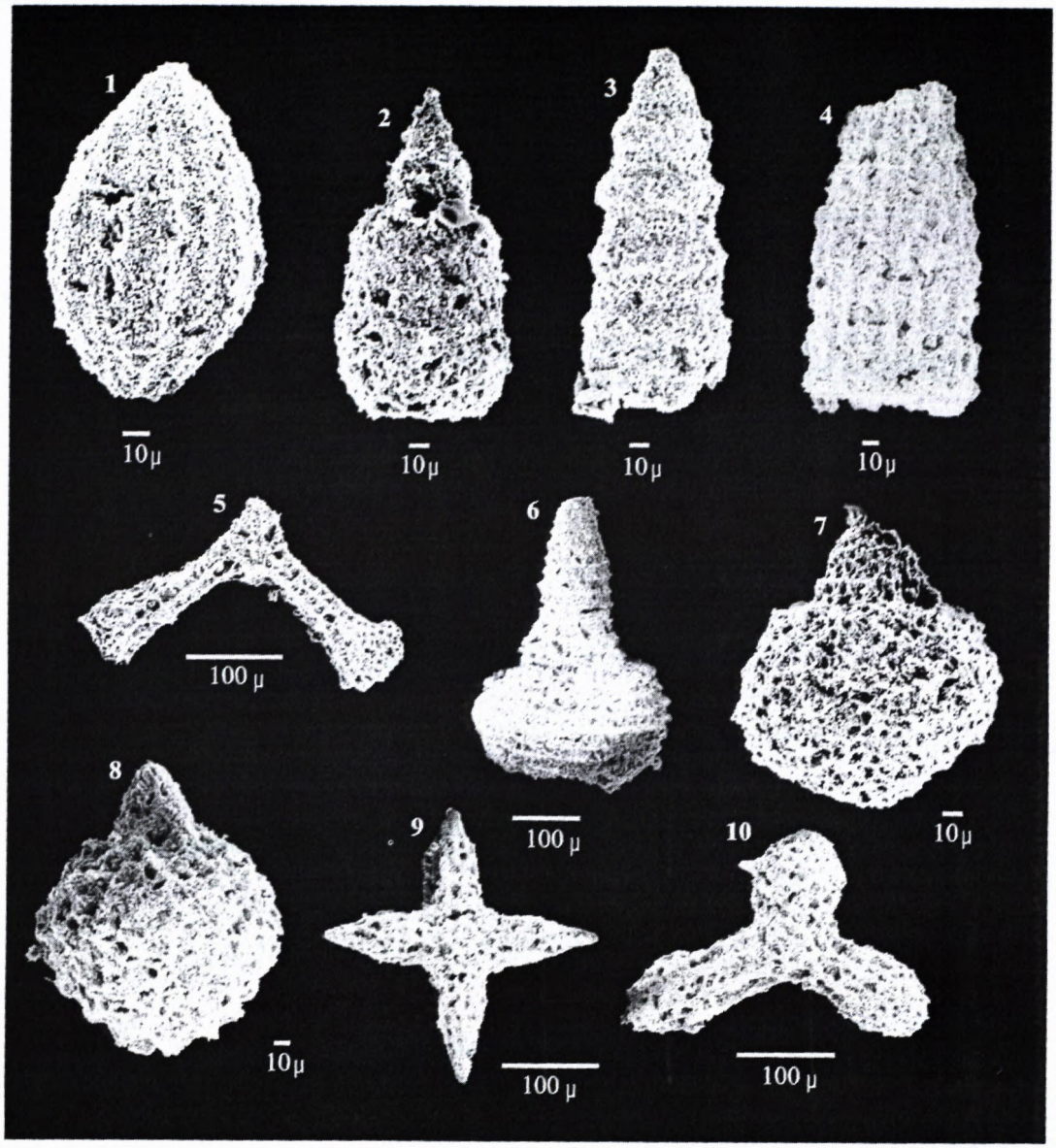

Fig. 8. (Sample ŠJ 25) 1– Protunuma japonicus Matsuoka et Yao – 8340, 2 – Eucyrtidiellum sp. –8339, 3 – Cinguloturris carpatica Dumitrică – 8336, 4 – Transhsuum maxwelli (Pessagno) – 8334, 5 – Angulobracchia sp. – 8337, 6 – Mirifusus guadalupensis Pessagno – 8331, 7 – Obesacapsula cf. morroensis (Pessagno) – 8338, 8 –- Sethocapsa funatoensis Aita – 8335, 9 – Pseudocrucella sanfilippoae (Pessagno) – 8333, 10 – Homoeoparonaella sp. – 8332.

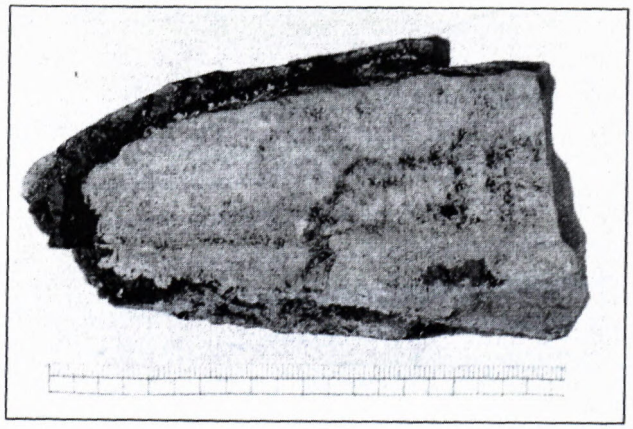

Fig. 9. Crust of manganese oxides (black) on carbonate rock with rhodochrosite. ŠJ 10.

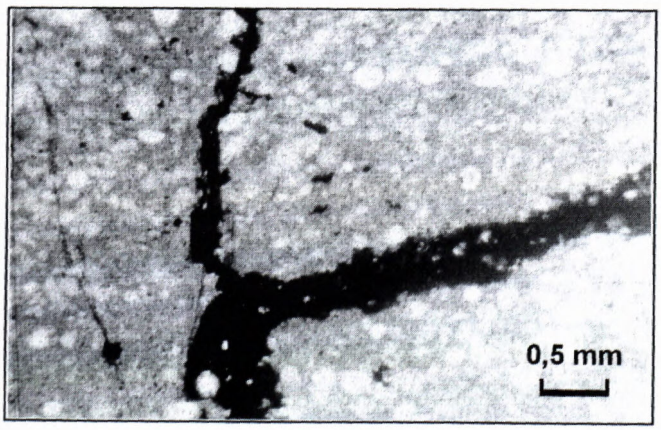

Fig. 10. Veinlet of manganese hydroxides (black). ŠJ 5, transmitted light, parallel nicols.

K, Mg, Mn, Na, Si and Sr. Natural and synthetic standards were applied on calibration of both systems: Al_2O_3, $BaSO_4$, Ca-wollastonite, Fe-hematite, K-orthoclase, MgO, Mn- rhodonite, Na-albite, SiO_2 and $SrTiO_3$. WDS analyses used 15 and 20 kV accelerating voltage, 15-18 nA beam current, and 10 to 20 seconds counting times according to total number of counts. Obtained counts were recalculated in oxides using PAP correction. Electron beam was focused on 2-5 micrometers. Chemical composition of minerals was calculated in the Minfile programme.

X-ray diffraction (XRD) analyses were made on a Philips PW 1710 diffractometer. Samples with high content of Fe were analysed by Co K_α radiation ($\lambda\alpha_1$ =1.78896 m^{-10}, $\lambda\alpha_2$ = 1.79285 m^{-10}) and Cu K_α radiation ($\lambda\alpha_1$ = 1.54060 m^{-10} $\lambda\alpha_2$ = 1.54439 m^{-10}) was used in case of other samples. Accelerating voltage of 35 kV and beam current of 20 mA were used in the range 4 to 60 ° 2Θ with shift 0.02 ° 2Θ.

Minerals

Rhodochrosite is dominant mineral of the carbonate layers in shale. Euhedral grains (from 0,01 to 0,05 mm in size) are replaced by manganese oxides and hydroxides and by iron hydroxides (Fig. 11). Marginal part of grains is mostly replaced. XRD (Tab. 2) and WDS confirmed rhodochrosite. Chemical composition shows variable and significant iron content in rhodochrosite reflecting mostly replacement by manganese and iron hydroxides and oxides (Tab. 3, Fig. 12). Pseudomorphs of todorokite and cryptomelane after rhodochrosite can be observed in some places.

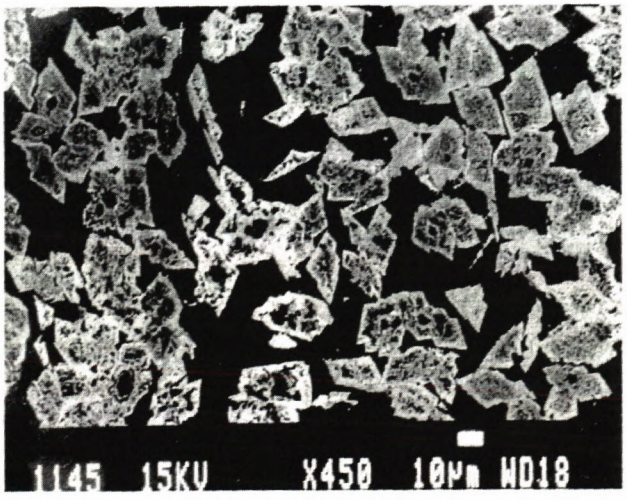

Fig. 11. Manganese and iron oxides and hydroxides (white) replace euhedral rhodochrosite (grey). ŠJ 9, scanning electron microscopy-back-scatter electron image (SEM-BEI).

Todorokite forms crusts (up to 1 mm thick) on rhodochrosite aggregates and fills fissures in them (up to 0.1 mm in thickness). Xenomorph distinctly anisotropic grains (10 to 50 µm in size) form darker core of concentric aggregates (0.02 to 0.03 mm in size) with rimming lighter romanèchite in reflected light (Fig. 13).

Tab. 2. X-ray diffraction of rhodochrosite

ŠJ 9		ŠJ 10		ŠJ 21		Rhodochrosite Mich 421		Quartz Mich 256	
d	I	d	I	d	I	d	I	d	I
4.255	2	4.271	1	4.255	1			4.24	5
3.628	1	3.644	1	3.649	3	3.65	7		
3.346	7	3.353	4	3.342	5			3.34	10
2.821	10	2.835	10	2.840	10	2.850	10		
2.458	1							2.45	5
2.373	1	2.375	1	2.375	1	2.389	4		
2.279	1							2.280	5
2.153	1	2.164	2	2.164	1	2.180	4		
1.983	1	1.984	2	1.988	2	1.990	5		
1.818	2	1.820	1	1.815	1	1.809	3		
				1.760	3	1.762	8		

Mich 421 and Mich 256 (XRD 421 and 256 in Michejev 1957)XRD

Tab.3 Chemical composition of carbonates

	Weight per cent					
Sample	CaO	MgO	FeO	MnO	CO_2	Total
ŠJ2	3.59	1.93	21.33	34.03	39.11	100.00
ŠJ9.1	0.57	2.09	34.15	24.40	38.79	100.00
ŠJ9.2	4.51	2.08	22.15	32.02	39.24	100.00
ŠJ9.3	3.30	2.01	23.31	32.29	39.09	100.00
ŠJ10.1	4.64	2.04	23.08	30.99	39.24	99.99
ŠJ10,2	3.50	1.97	22.42	32.99	39.11	99.99
ŠJ16.1	10.67	2.02	2.26	45.10	39.94	99.99
ŠJ16.2	3.03	2.00	29.95	25.99	39.03	100.00
ŠJ16.3	6.78	2.03	13.33	38.35	39.50	99.98
ŠJ16.4	2.31	2.08	32.02	24.62	38.97	100.00
ŠJ16.5	2.30	2.17	30.35	26.18	39.01	100.00
ŠJ20	1.63	1.47	27.47	30.69	38.75	100.00
ŠJ21.1	4.07	1.72	19.30	35.80	39.11	100.00
ŠJ21.2	4.80	2.04	19.10	34.77	39.27	100.00
ŠJ21.3	0.99	1.92	35.45	22.86	38.78	100.00
ŠJ21.4	4.50	2.08	19.66	34.51	39.25	100.00
ŠJ21.5	4.33	2.18	22.12	32.12	39.25	100.00
	Atomic proportion (to 3 oxygen)					
Sample	Ca	Mg	Fe	Mn	C	Total
ŠJ2	0.072	0.054	0.334	0.540	1.000	2.000
ŠJ9.1	0.012	0.059	0.539	0.390	1.000	2.000
ŠJ9.2	0.090	0.058	0.346	0.506	1.000	2.000
ŠJ9.3	0.066	0.056	0.365	0.512	1.000	2.000
ŠJ10.1	0.093	0.057	0.360	0.490	1.000	2.000
ŠJ10,2	0.070	0.055	0.351	0.523	1.000	2.000
ŠJ16.1	0.210	0.055	0.035	0.701	1.000	2.000
ŠJ16.2	0.061	0.056	0.470	0.413	1.000	2.000
ŠJ16.3	0.135	0.056	0.207	0.602	1.000	2.000
ŠJ16.4	0.046	0.058	0.503	0.392	1.000	2.000
ŠJ16.5	0.046	0.061	0.477	0.416	1.000	2.000
ŠJ20	0.033	0.041	0.434	0.491	1.000	2.000
ŠJ21.1	0.082	0.048	0.302	0.568	1.000	2.000
ŠJ21.2	0.096	0.057	0.298	0.549	1.000	2.000
ŠJ21.3	0.020	0.054	0.560	0.366	1.000	2.000
ŠJ21.4	0.090	0.058	0.307	0.545	1.000	2.000
ŠJ21.5	0.087	0.061	0.345	0.508	1.000	2.000

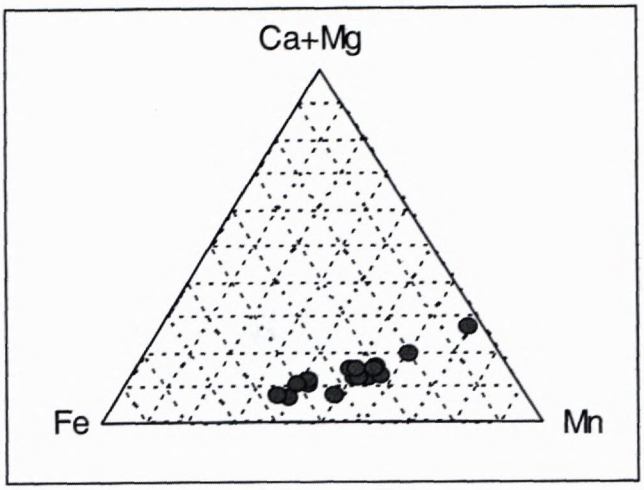

Fig. 12. Chemical composition of carbonates from Šarišské Jastrabie.

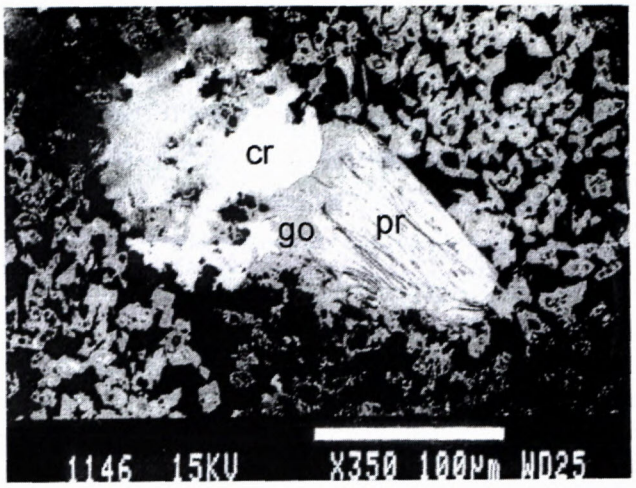

Fig. 15. Aggregate of pyrolusite (pr), cryptomelane (cr) and goethite (go) in radiolarite. ŠJ 16, SEM-BEI.

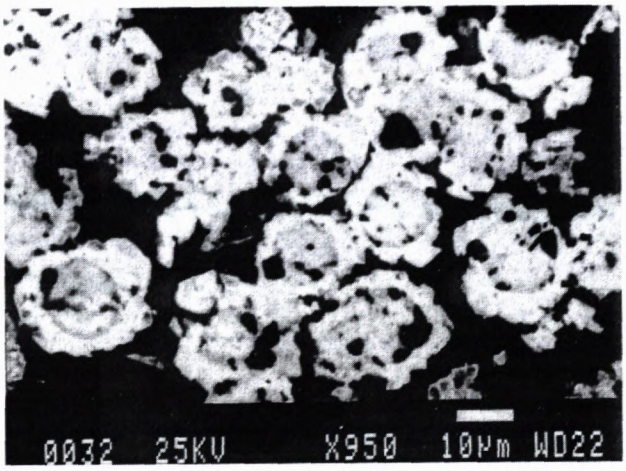

Fig. 13. Romanèchite forms external part of concentric aggregates (white) while in central part is todorokite (grey) in carbonate rock. ŠJ 1, SEM- BEI.

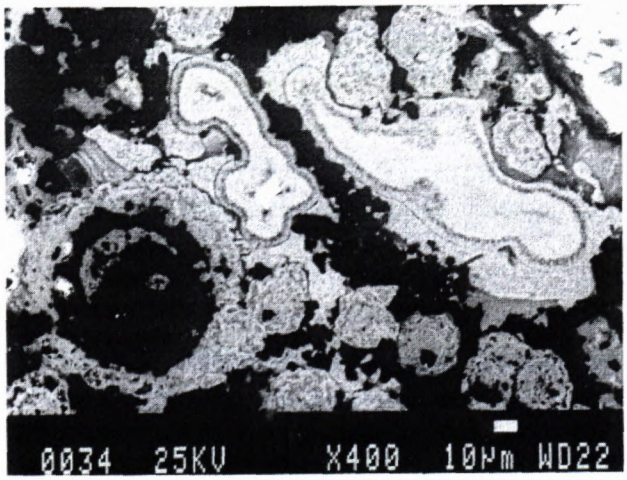

Fig. 14. Colloform cryptomelane (light grey) in todorokite (grey). Todorokite forms also colloform concentric aggregates. ŠJ 1, SEM- BEI.

XRD with maximum at 9.6 d suggests todorokite. Presence of characteristic calcium with manganese is also typical for todorokite (Tab. 4).

Romanèchite forms rims of concentric aggregates of todorokite and veinlets (from 0.03 to 0.1 mm in thickness). Increase of the barium content in WDS analyses in external zones of aggregates helped to distinguish romanèchite (Tab. 5). Characteristic peaks of romanèchite were distinguished also by XRD in fissure fillings in radiolarite chert.

Cryptomelane represents the lighter phase with higher relief in the reflected light than todorokite. It forms botryoidal colloform aggregates up to 0,1 mm in size (Fig. 14). It fills fissures in todorokite aggregates or veinlets. Veinlets of cryptomelane cut rhodochrosite and todorokite. It is less frequent than todorokite. Chemical composition of cryptomelane is characterised by total close to 100 wt. % and K_2O content ≥ 3 wt. % (Tab. 6).

Pyrolusite is easily distinguished in reflected light among other manganese minerals by high reflectivity, strong anisotropy (yellow-dark brown) and yellow colour. Elongated grains (0,01 to 0,1 mm long) form aggregates (Fig. 15). They form 0,1 to 0,2 mm thick crusts of layers with rhodochrosite, where elongated grains are oriented perpendicularly to the surface of bedding. Zoned crusts are often alternating with goethite. WDS analyses confirmed only low content of Fe and Ca below 1 weight per cent (Tab. 7).

Pyrite is disseminated in radiolarite chert and shale as irregular grains or framboidal pyrite (to 0,01 mm in size). Euhedral grains (0.01 to 0.05 m in size) form aggregates (to 0,5 mm in size) and veinlets in rock or in quartz veinlets.

Goethite and iron hydroxides intergrow very often with manganese hydroxides or they rim them (Fig. 15). They replace and rim rhodochrosite and pyrite forming often pseudomorphs after these two minerals. Grains and aggregates (0,01 to 0,3 mm in size) show variable Mn and Fe contents due to intimate intergrowths of iron and manganese hydroxides (Tab. 8).

Tab. .4. Chemical composition of todorokite

	Weight per cent							
Sample	MnO_2	CaO	MgO	SiO_2	Fe_2O_3	K_2O	BaO	Total
ŠJ1.1	84.58	2.70	0.71	0.11	0.00	1.46	0.00	89.56
ŠJ1.2	84.63	2.66	0.88	0.34	0.00	1.63	0.52	90.66
ŠJ1.3	84.93	2.67	0.91	0.32	0.00	1.78	0.30	90.91
ŠJ21.1	84.34	3.23	1.00	0.40	4.97	1.14	0.00	95.08
ŠJ24.1	87.44	2.42	1.58	0.03	0.23	1.76	0.00	93.46
ŠJ24.2	88.89	4.83	0.66	0.52	0.38	0.82	0.00	96.10
ŠJ24.3	86.11	3.28	0.78	2.62	1.02	1.18	0.00	94.99
ŠJ24.4	87.90	4.20	0.56	0.55	0.38	0.85	0.01	94.45
	Atomic proportion (to 7 oxygen)							
Sample	Mn	Ca	Mg	Si	Fe	K	Ba	Total
ŠJ1.1	3.354	0.166	0.061	0.006	0.000	0.107	0.000	3.694
ŠJ1.2	3.327	0.162	0.075	0.019	0.000	0.118	0.012	3.713
ŠJ1.3	3.327	0.162	0.077	0.018	0.000	0.129	0.007	3.719
ŠJ21.1	3.171	0.188	0.081	0.022	0.204	0.079	0.000	3.745
ŠJ24.1	3.324	0.143	0.130	0.002	0.010	0.124	0.000	3.731
ŠJ24.2	3.282	0.277	0.053	0.028	0.015	0.056	0.000	3.710
ŠJ24.3	3.184	0.188	0.062	0.140	0.041	0.081	0.000	3.696
ŠJ24.4	3.299	0.244	0.045	0.030	0.016	0.059	0.000	3.693

Tab. 5. Chemical composition of romanèchite

Sample	Weight per cent							
No	MnO_2	Fe_2O_3	MgO	SiO_2	K_2O	CaO	BaO	Total
ŠJ 1.1	79.91	0.80	0.23	0.43	0.70	1.99	6.19	90.25
ŠJ 1.2	80.20	2.67	0.27	0.43	0.86	2.20	4.52	91.14
ŠJ 1.3	82.10	1.89	0.35	0.19	1.05	2.74	3.42	91.73
Sample	Atomic proportion (to 10 oxygen)							
No	Mn^{+4}	Fe^{+3}	Mg	Si	K	Ca	Ba	Total
ŠJ1	4.698	0.051	0.029	0.036	0.076	0.181	0.206	5.278
ŠJ1	4.627	0.168	0.033	0.036	0.091	0.197	0.148	5.299
ŠJ1	4.672	0.117	0.043	0.016	0.110	0.242	0.110	5.309

Chemical composition of rocks

Radiolarite chert, shale and rhodochrosite intercalations are characterised by the different content of major elements (Tab. 9). Radiolarite chert can be distinguished by distinctly high SiO_2 content (over 90 wt. %). High Si/(Al+Fe) ratio suggests organic origin of radiolarite chert (Rangin et al. 1981). Shale shows increased Al_2O_3 content (around 10 wt. %), MgO and K_2O (3 to 8 wt. %). Manganese content in radiolarite chert as well as in shale is low (below 0,5 weight per cent of Mn). Halamič et al. (2001) give MnO to 0.51 wt. % in radiolarite chert from Croatia. Distinctly increased is manganese content in carbonate layers and boudinage (14 to 23 wt. % of Mn). Iron content does not correlate with manganese (Mn/Fe ratio varies from 0.98 to 3.88), reflecting bonds to iron hydroxides and less to rhodochrosite. Ca is higher (19 wt. %) in manganese ore with rhodochrosite and todorokite, where low iron content was found (sample ŠJ 1), suggesting the presence of primary Ca rhodochrosite before replacement by iron hydroxides. Presence of kutnahorite or calcite was not confirmed by XRD. Part of Ca may be bound to apatite as was confirmed by XRD and increased $P2O_5$ content (2,5 weight per cent). Carbonate layers and boudinage are characterised by increased CO_2 content (over 17 weight per cent), inorganic carbon (TIC over 4 weight per cent) and loss of ignition (LOI over 10 weight per cent).

Manganese ore shows similarly as in other occurrences in the Jurassic shale very low content of Co, Cu and Ni especially comparing to the ores in Jurassic limestone (Rojkovič, 2002). Ni+Co+Cu contents are slightly higher in shale and carbonate layers comparing to radiolarite chert. Cu is distinctly higher not only to radiolarite chert but also to carbonate layers. Local increase of Co and Ni can be observed in samples with higher pyrite content. Ti, Mg, K, Cr, V, B, Pb and Zr contents are distinctly higher in shale and carbonate layers comparing to radiolarite chert. Mg, K, Cr and V are related to Al_2O_3 content mostly in clay minerals (illite and chlorite) similarly as in shale accompanying radiolarite chert in Mino-Tamba, Japan (Kakuwa, 1986). Ti, B and Zr contents in the stud-

Tab. 6. Chemical composition of cryptomelane

No	Weight per cent					
	K_2O	MnO_2	Fe_2O_3	SiO_2	CaO	Total
ŠJ 1.1	3.26	94.69		0.32	0.73	99.01
ŠJ 1.2	3.05	95.14		0.00	0.00	98.18
ŠJ 1.3	3.20	95.56		0.28	0.87	99.91
ŠJ16.1	2.51	96.59	0.59		0.32	100.01
ŠJ16.2	2.60	96.56	0.56		0.28	100.00
ŠJ16.3	2.46	96.55	0.70		0.29	100.00
ŠJ16.4	3.13	95.17	0.60		0.31	99.21
ŠJ16.5	2.54	95.99	0.66		0.27	99.46
ŠJ16.6	3.08	94.98	0.80		0.43	99.30
ŠJ 20.1	3.38	94.38	0.28	0.05	1.43	99.52
ŠJ 20.2	3.10	94.49	0.24	0.05	1.21	99.09
ŠJ 20.3	2.61	92.95	0.32	0.06	1.92	97.86
ŠJ 20.4	2.83	94.34	0.62	0.07	1.74	99.60
ŠJ 24.1	2.91	94.01	0.18	0.05	1.13	98.28
ŠJ 24.2	3.23	95.82	0.24	0.10	1.13	100.52
No	Atomic proportion (to 16 oxygen)					
	K	Mn	Fe	Si	Ca	Total
ŠJ 1.1	0.496	7.791		0.038	0.093	8.418
ŠJ 1.2	0.466	7.884		0.000	0.000	8.350
ŠJ 1.3	0.482	7.792		0.033	0.110	8.417
ŠJ16.1	0.376	7.847	0.052		0.041	8.315
ŠJ16.2	0.390	7.848	0.049		0.035	8.323
ŠJ16.3	0.369	7.843	0.062		0.037	8.310
ŠJ16.4	0.475	7.821	0.054		0.039	8.389
ŠJ16.5	0.383	7.843	0.059		0.034	8.319
ŠJ16.6	0.468	7.802	0.072		0.055	8.396
ŠJ 20.1	0.513	7.756	0.025	0.006	0.182	8.482
ŠJ 20.2	0.471	7.783	0.022	0.006	0.155	8.436
ŠJ 20.3	0.402	7.747	0.029	0.007	0.248	8.432
ŠJ 20.4	0.428	7.733	0.055	0.008	0.221	8.446
ŠJ 24.1	0.446	7.798	0.016	0.006	0.145	8.411
ŠJ 24.2	0.484	7.780	0.021	0.012	0.142	8.440

ied samples may reflect the presence of clastic minerals in sediments like rutile, tourmaline and zircon. Layers and boudinage with rhodochrosite show the highest Sr content bound to carbonates.

Distribution of the rare earth elements (REE) shows only slight positive Ce anomaly and REE contents similar to other occurrences in the Jurassic shale of the Western Carpathians (Borinka, Lednické Rovne and Zázrivá). Slight positive Ce anomaly suggest terrigenous and not hydrothermal source of manganese associated with volcanic activity (Fig. 16). La/Ce=0.28 is similar like in other Jurassic shale (0.26) and it is distinctly different from ratio La/Ce=2.8 of seawater characteristic for hydrothermal accumulation of manganese on the sea bottom (Toth, 1980). Small positive Eu anomaly reflects continental source of material and exclude hydrothermal manganese accumulation with typical negative Ce anomaly (Shimizu & Masuda, 1977, Matsumoto et al., 1985, Usui et al., 1997, Kuhn et al., 1998).

Tab. 7. Chemical composition of pyrolusite

No	Weight per cent			
	MnO_2	Fe_2O_3	CaO	Total
ŠJ 9.1	98.22	0.39	0.49	99.10
ŠJ 9.2	98.00	0.83	0.42	99.25
ŠJ 9.3	98.18	0.44	0.48	99.09
ŠJ 16.11	97.91	1.49	0.11	99.51
ŠJ 16.2	97.73	1.74	0.17	99.64
ŠJ 16.3	98.75	0.77	0.18	99.70
ŠJ 21.1	98.27	0.38	0.80	99.45
ŠJ 21.2	98.25	0.38	0.71	99.34
No	Atomic proportion (to 2 oxygen)			
	Mn	Fe	Ca	Total
ŠJ 9.1	0.993	0.004	0.008	1.005
ŠJ 9.2	0.990	0.009	0.007	1.006
ŠJ 9.3	0.993	0.005	0.008	1.005
ŠJ 16.11	0.987	0.016	0.002	1.005
ŠJ 16.2	0.984	0.019	0.003	1.006
ŠJ 16.3	0.992	0.008	0.003	1.004
ŠJ 21.1	0.991	0.004	0.013	1.007
ŠJ 21.2	0.991	0.004	0.011	1.007

Origin

Chemical composition, microscopic observation as well as geological position of manganese ore suggested according to Ilavský (1955) secondary origin of ore by mobilization of disseminated manganese mineralization from the radiolarite chert to the basal part of radiolarite overlying impermeable shale.

Primary manganese mineralization is bound to shale according to recent observations. We have similar situation as in other occurrences of manganese mineralization in the Pieniny Klippen Belt like Lednické Rovne and Zázrivá (Polák, 1955, Čillík, 1963). Microbial suboxic diagenesis and reduction of hydrogenous Mn^{+4} hydroxides by organic carbon was significant for origin of manganese carbonates (Roy, 1992, Öztürk & Hein, 1997, Gutzmer & Beukes, 1998). We assume formation of rhodochrosite layers by metasomatic replacement of marl during diagenesis. Reduction of sulphates was also important during the early diagenesis (Fan et al., 1999). Reduction of sulphates is dominant in sediments with lower Mn content (Veto et al., 1997). Pyrite formed most probably during diagenesis was found in radiolarite chert as well as in shale.

Supergene processes remobilized later manganese. Crusts of manganese oxides and hydroxides accompanied by iron hydroxides were formed in shale along bedding and perpendicular fissures. Pyrite was oxidized and sulphate solutions were formed. Important role of pyrite oxidation is known in Urkút deposit in Hungary where manganese and iron were leached from marl with radiolarite chert and mobilized by acid solutions (Szabó & Grasselly, 1980). Acid solutions could mobilize manganese also from shale with rhodochrosite in Šarišské

Tab. 8. Chemical composition of Fe-Mn hydroxides

No	Weight per cent						
	Fe_2O_3	MnO_2	Al_2O_3	SiO_2	CaO	K_2O	Total
SJ 10.1	40.59	45.73	0.72	1.50	0.42	0.08	89.04
SJ 10.2	46.52	38.87	0.85	1.71	0.41	0.06	88.42
SJ 16	80.53	8.37			0.08	0.02	89.00
ŠJ 21.1	30.34	65.38		0.87	0.71	0.29	97.59
ŠJ 21.2	69.63	14.50		3.29	0.46	0.08	87.96
	Atomic proportion						
No	Fe	Mn	Al	Si	Ca	K	Total
SJ 10.1	0.470	0.486	0.013	0.023	0.007	0.002	1.000
SJ 10.2	0.538	0.413	0.015	0.026	0.007	0.001	1.000
SJ 16	0.912	0.087			0.001	0.000	1.000
ŠJ 21.1	0.326	0.645		0.012	0.011	0.005	1.000
ŠJ 21.2	0.790	0.151		0.050	0.007	0.002	1.000

Tab. 9. Chemical composition of manganese ore and rocks

Sample	ŠJ 1	ŠJ 5	ŠJ 8	ŠJ 9	ŠJ 10	ŠJ 14	ŠJ 15
SiO_2	33.12	93.47	65.14	27.94	32.87	91.36	69.92
TiO2	0.18	0.09	0.44	0.13	0.12	0.09	0.34
Al_2O_3	8.41	2.12	10.90	2.72	2.01	2.19	9.71
FeO	2.56						
Fe_2O_3	2.38	0.78	3.41	23.29	20.08	0.94	4.41
MnO	18.27	0.29	0.02	20.59	29.72	0.61	0.09
MgO	0.94	0.24	2.73	1.51	0.15	0.08	3.23
CaO	19.11	0.27	0.38	1.89	1.31	0.24	0.73
Na_2O	0.02	0.12	1.37	0.88	0.86	1.80	1.39
K_2O	0.03	0.48	8.29	0.81	0.80	0.39	3.41
P_2O_5	2.56	0.07	0.03	0.03	0.04	0.06	0.24
H_2O-	0.01	0.20	0.93	0.51	2.09	0.35	0.75
LOI	14.56	1.46	5.89	19.30	9.52	1.36	5.34
Total	102.15	99.59	99.52	99.62	99.57	99.46	99.55
B	2	46	136	357	41	47	94
Ba	15	213	215	127	42	324	206
Co	106	16	23	30	21	15	16
Cr	24	85	101	23	59	21	80
Cu	2	22	76	17	31	26	84
La	61	102	67				88
Mo	13	2	~1				~1
Ni	58	26	33	48	20	24	26
Pb	38	15	31	21	45	6	20
Sr	227	31	86	192	>500	65	84
V	50	12	88	17	20	13	58
Y	18	17	21	37	31	26	32
Zr	58	21	98	220	184	25	80
TC%	4.56	traces	0.2	5.11	0.12	0.1	0.28
TOC%	0.1	traces	0.16	0.2	0.12	st	0.2
TIC%	4.46	traces	0.04	4.91	traces	0.1	0.08
CO2 carb			0.146	17.97	traces	0.37	0.293
Fe tot	3.65	0.55	2.39	16.29	14.04	0.66	3.08
Mn	14.15	0.22	0.02	15.95	23.02	0.47	0.07
Mn/Fetot	3.88	0.40	0.01	0.98	1.64	0.72	0.02
NiCoCu	166	64	132	95	72	65	126
rock	Mn-ore	radio-larite	shale	Mn-ore	Mn-ore	radio-larite	shale

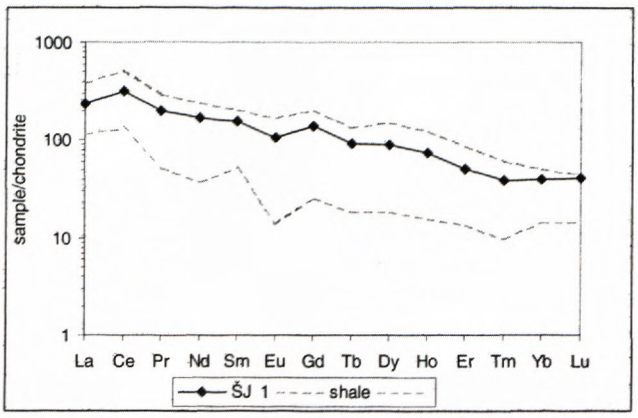

Fig. 16. Distribution of REE in sample ŠJ1. Field of manganese ores in Jurassic shale of the Western Carpathians is marked with dashed line.

Jastrabie. Their circulation facilitated tectonic contact of shale and radiolarite chert. Solutions could circulate from shale into sunken radiolarite chert close to the tectonic contact, where manganese hydroxides and oxides were formed.

The manganese mineralization in the radiolarite chert fills fissures along and across bedding and its origin is secondary. For this reason a dividing of radiolarite sequence to manganese radiolarite of the Sokolica Radiolarite Formation and to overlying radiolarite of the Czajakowa Radiolarite Formation by Birkenmajer (1977) is doubtful.

Acknowledgements:

We thank for the analyses of part of rocks and minerals to Ľ. Puškelová from Geological Institute of Slovak Academy of Sciences and to D. Ozdín from Geological Survey of the Slovak republic. The study was supported by grants 160 of VTP GP and 1/7293/20 of VEGA. The manuscript benefited from reviews by P. Konečný and M. Potfaj.

References

Baumgartner, P. O., Bartolini, A., Carter, E., Conti, M., Cortese, G., Danelian, T., De Wever, P., Dumitrică, P., Dumitrică-Jud, R., Goričan, S., Guex, J. M., Hull, D., Kito, N., Marcucci, M., Matsuoka, A., Murchey, B., O'Dogherty, L., Savary, J., Vishnevskaja, V., Widz, D.& Yao, A., 1995: Middle Jurassic to Early Cretaceous radiolarian biochronology of Tethys based on Unitary Associations. In: Baumgartner P.O., O'Dogherty L., Goričan S., Urquhart E., Pillevuit A. & De Wever P. (Eds.): Middle Jurassic to Lower Cretaceous Radiolaria of Tethys: Occurrences, Systematics, Biochronology. Mémoires de Géologie (Lausanne), 23, 1013-1048

Birkenmajer, K. 1954: Sprawozdanie z badan geologicznych wykonanych w pieninskim pasie skałkowym w latach 1950 - 1951, Inst. Geol., Biul., vol. 86, 81-115.

Birkenmajer, K. 1958: Przewodnik geologiczny po pieninskim pasie skałkowym, I, Wydawnictwa Geologiczne, 1-135.

Birkenmajer, K., 1977: Jurassic and Cretaceous lithostratigraphic units of the Pieniny Klippen Belt, Carpathians, Poland. Studia geol. Polonica, 45, 1-159.

Bonatti, E., Zerbi, M., Kay, R. & Rydell, H., 1976: Metalliferous deposits from the Apennine ophiolites: Mesozoic equivalents of modern deposits from oceanic spreading centers. Geol. Soc. Amer. Bull., 87, 83-94.

Crerar, D. A., Namson, J., Chyi, M. S., Williams, L. & Feigenson, M. D., 1982: Manganiferous cherts of the Franciscan Assemblage: I. General geology, ancient and modern analogues, and implications for hydrothermal convection at oceanic spreading centers. Econ. Geol., 77, 519-540.

Čilík, I., 1963: Ložisko mangánovej rudy pri Zázrivej. Geologické práce, Zprávy 29, 125-132.

Fan, D. L., Ye, J., Yin, L. M. & Zhang, R. F., 1999: Microbial processes in the formation of the Sinian Gaoyan manganese carbonate ore, Sichuan Province, China. Ore Geology Reviews, 15, 79-93.

Gutzmer, J. & Beukes, N. J., 1998: The manganese formation of the Neoproterozoic Penganga Group, India – revision of an enigma. Econ. Geol., 93, 1091-1102.

Halamič, J., Marchig, V. & Goričan, Š., 2001: Geochemistry of Triassic radiolarian cherts in north-western Croatia. Geol.Carpath., 52, 327-342.

Ilavský, J. 1955: Výskyt mangánovej rudy v bradlovom pásme pri Šarišskom Jastrabí. Geol. zborník SAV VI, 1-2, Bratislava, 119-127.

Kakuwa, Y., 1986: Petrography abd geochemistry of argillaceous rocks associated with Triassic to Jurassic bedded chert of the Mino-Tamba Terrane. Scient. papers College of arts and Science, Tokyo, 36, 137-162.

Kuhn ,T., Bau, M., Blum, N. & Halbach, P., 1998: Origin of negative Ce anomalies in mixed hydrothermal-hydrogenetic Fe-Mn crusts from the Central Indian Ridge. Earth and Planet. Sci. Letters, 163, 207-220.

Matsumoto, R., Minai, Y. & Iijima, A., 1985: Manganese content, Cerium anomaly, and rate of sedimentation as clues to characterize and classify deep sea sediments. In: „Advances in Earth and Planetary Sciences, Formation of Oceanic Margin". Terra Sci. Pub., Tokyo, 913-939.

Michejev, V. I., 1957: Rentgenometričeskij opredelitel' mineralov. Gosgeoltechizdat, Moskva, 1-868.

Myczyński, R, 1973: Middle Jurassic stratigraphy of the Branisko succesion in the vicinity of Czorstyn, Pieniny Klippen Belt, Carpathians, Stud. Geol. Polon., 42, 1-122.

Nemčok, J., 1973: Vysvetlivky ku geologickej mape 1 : 25 000 Kamenica Ľubotín, Čiatková záverečná správa, GÚDŠ, 1-48.

Nemčok, J., 1990: Geologická mapa Pienin, Čergova, Ľubovnianskej a Ondavskej vrchoviny, GÚDŠ.

Nemčok, J., Zakovič, M., Gašparíková, V., Ďurkovič, T., Snopková, P., Vrana, K. & Hanzel, V., 1990: Vyvetlivky ku geologickej mape Pienin, Čergova, Ľubovnianskej a Ondavskej vrchoviny, 1 : 25 000, GÚDŠ, 1-131.

Ožvoldová, L. & Frantová, L., 1997: Jurassic Radiolarites from the eastern part of the Pieniny Klippen Belt (Western Carpathians). Geol. Carpath., 48, 1, 49-61.

Öztrük, H. & Hein, J. R., 1997: Mineralogy and stable isotopes of black shale hosted manganese ores, Southwestern Taurides, Turkey. Economic Geology, 92, 733-744.

Polák, S., 1955: Primárna manganorudná zóna ložiska v Lednickom Rovnom. Geologické práce, Zprávy 2, Bratislava, 48-59.

Rangin, C., Steinberg, M. & Bonnot-Courtois, C. 1981: Geochemistry of the Mesozoic bedded chert of Central Baja California (Vizcaino-Cedros-San Benito): Implications for paleogeographic reconstruction of an old oceanic basin. Earth Planet. Sci. Lett. 54, 313-322.

Rojkovič, I., 2002: Manganese mineralization in Jurassic sequences, Slovakia. Geol. Carpath., 53, spec. issue, 87-89.

Roy, S., 1992: Environments and Processes of Manganese Deposition. Econ. Geol. 87, 1218-1236.

Shimizu, H. & Masuda, A., 1977: Cerium in chert as an indicator of marine environment of its formation. Nature, 266, 346-348.

Szabó, Z. G. & Grasselly, 1980: Genesis of manganese oxide ores in the Úrkút basin Hungary In: Varentsov I. M. & Grassely G. (Eds.): Geology and geochemistry of manganese, Akadémiai Kiadó, Budapest, Volume II, 223-236.

Toth, J. R., 1980: Deposition of submarine crusts rich in manganese and iron. Geol. Soc. Amer. Bull., 91, 44-54.

Usui, A., Bau, M. & Yamazaki, T., 1997: Manganese microchimneys buried in the Central Pacific pelagic sediments: evidence of intraplate water circulation? Marine Geology, 141, 269-285.

Veto, I., Demeny, A., Hertelendi, E. & Hetenyi, M., 1997: Estimation of primary productivity in the Toarcian Tethys - A novel approach based on TOC, reduced sulphur and manganese contents. Palaeogeography, Palaeoclimatology, Palaeoecology, 132, 355-371.